Polar Data Journal, Vol. 1, 1–16, October 2017

Surface elevations on Qaanaaq and Bowdoin Glaciers in northwestern Greenland as measured by a kinematic GPS survey from 2012–2016

Shun TSUTAKI[1,2,3]*, Shin SUGIYAMA[1] and Daiki SAKAKIBARA [1,4]

[1] Institute of Low Temperature Science, Hokkaido University, Nishi-8, Kita-19, Kita-ku, Sapporo, Hokkaido 060-0819.

[2] Arctic Environment Research Center, National Institute of Polar Research, Research Organization of Information and Systems, 10-3, Midori-cho, Tachikawa, Tokyo 190-8518.

[3] Earth Observation Research Center, Japan Aerospace Exploration Agency, 2-1-1, Sengen, Tsukuba, Ibaraki 305-8505.

[4] Arctic Research Center, Hokkaido University, Nishi-11, Kita-21, Kita-ku, Sapporo, Hokkaido 001-0021.

*Corresponding author. Shun Tsutaki (tsutshun@frontier.hokudai.ac.jp)

(Received June 14, 2017; Accepted September 19, 2017)

Abstract: Kinematic GPS measurements provide in-situ data crucial for measuring the surface elevation change of glaciers. Owing to their accuracy, which is generally better than half meter, surface elevations derived from kinematic GPS surveys are useful and essential for generating precise digital elevation models (DEMs) and evaluating geometry changes of glaciers. We present a surface elevation data set derived from kinematic GPS measurements covering the lower 5 km of Qaanaaq and Bowdoin Glaciers in northwestern Greenland. The data includes elevations over ice-free terrain nearby the glaciers, important for calibrating remote sensing data. More than 600,000 GPS survey data points were processed to produce a 1-m resolution mesh grid of elevation data in a CSV file format. Based on our error analysis, the accuracies of the elevation data are better than 0.2 and 0.3 m in horizontal and vertical directions, respectively. This dataset can be utilized to investigate glacier surface elevation changes by making comparison with DEMs obtained in the past, and from future remote sensing and in-situ observations.

1. Background & Summary

We present a surface elevation data set for Qaanaaq and Bowdoin Glaciers in northwestern Greenland, derived from GPS kinematic measurements in 2012–2016. The data covers the lower 5 km of the glaciers and nearby ice-free terrain with a spatial resolution of 1 m.

The Greenland ice sheet is losing mass because of increased amounts of surface melting and ice

discharge from marine-terminating outlet glaciers. Mass loss has also increased at glaciers and ice caps (GICs) along the coastal regions of Greenland, which are physically separated from the ice sheet. The mass loss in the Greenland ice sheet and GICs attracts attention as it has affected recent sea level rise[1,2]. Repeated surface elevation surveys by satellite-based laser/radar altimetry revealed recent widespread ice thinning along the coast of the ice sheet and GICs[3,4]. Ice thinning in Greenland is inhomogeneous in space and time[5]. For example, particularly large mass loss is observed in the fast-flowing marine-terminating outlet glaciers of the ice sheet[6].

Widespread thinning of marine-terminating outlet glaciers and GICs in Greenland has been revealed by satellite and airborne altimetry[7-9], as well as photogrammetric analysis of stereo-pair aerial photographs and satellite images[10-13]. These techniques are powerful tools to cover a relatively large space. However, the accuracy of these measurements relies on the footprint size of laser/radar signals, spatial coverage of satellite tracks, and the spatial resolutions of images. Accurate coordinates for ground control points (GCPs) are needed to perform the photogrammetric analysis. GCPs are also necessary for measuring the volume change of a glacier by differencing DEMs, because DEMs obtained by different techniques should be corrected for biases in the vertical direction[14,15].

Although spatial and temporal coverage are limited, kinematic GPS measurements provide surface elevation with a relatively high accuracy within half meter. Measurements on glaciers have been used for GICs in Svalbard[16,17], the Canadian Arctic[18] and Norway[19]. GPS data from ice-free terrain are often used to GCPs and calibrate DEMs, as reported for high Arctic GICs[20]. In the Greenland ice sheet, kinematic GPS measurements were utilized around ice core drilling sites to produce local surface topography maps[21,22]. However, kinematic GPS measurements data is sparse on and around marine-terminating outlet glaciers and GICs.

To investigate the mass loss of glaciers and ice caps in northwestern Greenland, intensive field research activities have been carried out since 2012 at Qaanaaq Glacier, an outlet glacier of Qaanaaq Ice Cap, and Bowdoin Glacier, a marine-terminating outlet glacier of the Greenland ice sheet (Fig. 1). This activity was a part of the Green Network of Excellence (GRENE) Arctic Climate Change Research Project and the Arctic Challenge for Sustainability (ArCS) Project[13,23-25]. Marine-terminating outlet glaciers of the ice sheet and GICs in this region are losing mass at an increasing rate[2,11,12], which is consistent with the acceleration of the ice mass loss reported in northwestern Greenland since 2005 (ref. 10). Thus, it is crucial to study marine-terminating outlet glaciers and GICs in this region to understand the mechanisms behind the recent increase in mass loss. To study recent surface elevation change, kinematic GPS measurements have been carried out at Qaanaaq and Bowdoin Glaciers and peripheral ice-free terrain since 2012. Although the spatial coverage of our ground based measurement is limited, the data set covers the most significantly changing lower part of the glaciers. By comparing our elevation data with those measured in the past (and going forward in the future), it is possible to measure surface elevation changes with a high degree of accuracy and

high spatial resolution (e.g. <2 m). Furthermore, data obtained on ice-free terrain serve as GCPs for remote sensing data analysis. Bowdoin Glacier was selected as the study site because of its recent rapid retreat, acceleration and thinning[13,24]. Bowdoin and Qaanaaq Glaciers are suitable for field measurements because of their relatively safe ice-surface conditions and proximity to Qaanaaq Village and Qaanaaq Airport. The aim of this paper is to provide surface elevation data measured at these glaciers and peripheral ice-free terrain from a kinematic GPS survey over 2012 to 2016. GPS coordinates obtained with different GPS devices and spatial resolutions were homogenized by interpolating the data for 1 × 1 m grid points with an accuracy of <0.3 m in horizontal and vertical directions. The data should also serve for DEM generation as well as investigations of the dynamic behavior of glaciers. The surface elevation data is made available in a CSV file format with WGS 84 geographic and Universal Transverse Mercator (UTM) coordinate systems.

2. Study Site

Qaanaaq Glacier (77°30′ N, 69°11′ W) is one of the outlet glaciers of Qaanaaq Ice Cap located 3 km from Qaanaaq Village in northwestern Greenland (Fig. 1). The glacier covers an elevation range of 207–1128 m a.s.l. and an area of 9.57 km^2 in 2014 (ref. 25). Surface elevation, ice thickness, surface mass balance, ice velocity and subsurface ice temperature measurements have been carried out near the flowline of the glacier since 2012 (ref. 23, 25). The change in surface elevation of GICs in northwestern Greenland was measured by differencing satellite-derived DEMs and repeated laser altimetry measurements. For example, the mean elevation change rate over the Qaanaaq Ice Cap was −1.8 ± 0.1 m a^{-1} from 2007 to 2009 (ref. 12), which is significantly greater than the mean rate (−0.6 ± 0.1 m a^{-1}) over the all GICs in northwestern Greenland for the 2003–2008 period[2]. We carried out surface elevation measurements in the summers of 2012–2015 along a survey route from the glacier terminus to an elevation of 1100 m a.s.l. The ice-free area between the glacier and Qaanaaq Village was also surveyed.

Bowdoin Glacier is a marine-terminating outlet glacier located 30 km northeast from Qaanaaq (77°41′ N, 68°35′ W) (Fig. 1). Approximately 20 km long, fast flowing ice bifurcates into Bowdoin Glacier and land-terminating Tugto Glacier 10 km from the terminus. Bowdoin Glacier flows southward and discharges ice into Bowdoin Fjord through a 3 km-wide calving front at a rate of approximately 440 m a^{-1} in 2013 (ref. 24). In Bowdoin Glacier, changes in terminus position, ice thickness and bed geometry were reported based on combined field and satellite observations[24]. The glacier front position had been stable since 1987 until it went into a rapid retreat in 2008 (ref. 24). Surface elevation change of Bowdoin Glacier was measured by differencing satellite-derived DEMs and repeated laser/radar altimeter measurements. The results showed thinning rates of −4.1 ± 0.4 m a^{-1} for 2007–2010 (ref. 13) and −5.0 ± 0.1 m a^{-1} for 2009–2012 (ref. 5). These rates are significantly greater than neighboring marine-terminating outlet glaciers in the Qaanaaq region[5]. Kinematic GPS

measurements were carried out in the summers of 2013–2016 on the lower 5 km of the glacier and ice-free area near the eastern margin of the glacier.

3. Methods

3.1. GPS Survey

Surface elevations were measured from 26 to 29 July 2012, from 20 to 21 July 2013, from 17 June to 3 August 2014 and 30 July 2015 on Qaanaaq Glacier (Table 1). On Bowdoin Glacier, the kinematic GPS survey was carried out from 7 to 12 July 2013, from 12 to 25 July 2014, from 9 to 16 July 2015 and from 9 to 19 July 2016 (Table 1). We used dual frequency carrier-phase GPS receivers and antennae (Leica, System 1200 and GNSS Technology Inc., GEM-1) to measure three-dimensional coordinates of the glacier and land surfaces. One of the receivers was situated on a stable roof of shed in Qaanaaq Village as a reference station for the survey at Qaanaaq Glacier (Figs 2a and 3). A GPS antenna was mounted on a stable tribrach and situated above a marker painted on the roof. A reference station at Bowdoin Glacier was situated on a stable boulder on the eastern flank of the glacier (Figs 2b and 4). The same type of tribrach stabilized with rocks was used to install a GPS antenna on the boulder, which was painted to show the accurate location of the tribrach. For both reference stations, electrical power was supplied from a battery (12V and 7.2Ah; GS YUASA, PXL12072) connected to a solar panel (Shell Solar Japan, SJJ20) (Fig. 2b). GPS data were recorded at a sampling rate of 1 s. On the glacier and ice-free terrain, GPS data were recorded every 1 s by a surveyor moving with a rover receiver. For the field campaign in 2012 and 2013, GPS antenna was mounted on the top of a 2-m-long pole (Table 1, Fig. 2c). In this paper, this survey method is referred as the pole method. Observer made a brief stop with intervals of <50 meter and recorded data for 20–30 s. For the measurements in 2014–2016, observers carried a frame pack with a GPS receiver and antenna fixed on it (Table 1, Fig. 2d). Measurements were carried out without stop. We refer to this survey method as the frame pack method. The height of the antenna above the glacier and land surfaces was measured before and after the survey. The frame pack method is less time consuming than the pole method, while its survey accuracy is sufficient for our purpose. Therefore, a greater number of measurements over a large area is possible with this method. Moreover, the frame pack method is efficient to re-survey the same coordinates, which is advantageous for the purposes of evaluating surface elevation change. For these reasons, we have employed the frame pack method since 2014. In 2012, a GPS survey on Qaanaaq Glacier was made along a route spanning mass balance stakes installed along the central flowline in the lower 5 km (Fig. 3). A survey was performed along additional routes in the later years, dependent on field activities each year. On Bowdoin Glacier, one longitudinal and three transverse survey routes were taken in the lower 3 km in 2013 (Fig. 4). The routes were determined such that they cover our area of interest within a distance of several kilometers. The density of crevasses was taken into account for safety during the measurements. Additional routes were surveyed in 2014–2016, shown in Fig. 4. By using the

coordinates measured in the first year, the same survey points were re-surveyed using an additional single point positioning GPS (Garmin, eTrex Vista HCx). In addition to the surveys on the glaciers, we measured surface elevation off the glaciers to collect GCPs. The total number of data points obtained over the periods from 2012 to 2016 were 172,633 at Qaanaaq Glacier and 437,184 at Bowdoin Glacier.

3.2. Data Processing

Post processing of the GPS data used the following steps: conversion of raw data to RINEX format, processing for coordinates in a kinematic mode and generation of 1-m mesh elevation data. In this section, we describe details of this procedure.

GPS data recorded at reference and rover stations were converted to a RINEX file format with converter software JPS2RIN[26]. We used open source GPS software RTKLIB[27] for post-processing the GPS data. L1 and L2 frequency data were processed with a 15° elevation mask, by correcting ionospheric and tropospheric effects by applying broadcast ionospheric and Saastamoinen models. First, we determined the three-dimensional coordinates of the reference stations as below. (1) For the Qaanaaq reference station, we processed GPS data recorded from 29 June to 4 August 2013 in precise point positioning (PPP) static mode. The computation was performed for every 3-day period, and an average of the processed data (n = 9) was taken as the reference coordinates. (2) GPS data recorded at the Bowdoin reference station were processed in a static mode with those from the Qaanaaq reference station for every 1-h segment from 5 to 27 July 2013. After excluding float solutions (>10 mm standard deviation), coordinates of the Bowdoin reference station were determined by averaging the results (n = 314). Coordinates were represented in the WGS 84 geographic coordinate system with ellipsoid height. The coordinates of the GPS reference stations in Qaanaaq Village and Bowdoin Glacier are summarized in Table 2.

We generated a 1-m mesh grid surface elevation data following procedures give below. (1) All GPS data were post-processed in a kinematic mode with RTKLIB to obtain coordinates relative to the reference stations. Coordinates were computed for every second, irrespective of the survey method. (2) Float solutions (standard deviations of >0.09 m in horizontal and >0.18 m in vertical directions) were excluded from the analysis. Accordingly, 61% of the data points made it through for use in these subsequent analyses. (3) The height of the GPS antenna was subtracted from the elevation data. Horizontal coordinates were transformed to the Universal Transverse Mercator projection (UTM, zone and latitude bands 19X, WGS 84 reference system). (4) Data on the glacier and land surfaces were distinguished based on elevation change, satellite images and photographs taken at the glacier margin during the field campaign. This process was manually carried out on orthorectified Panchromatic Remote-sensing Instrument for Stereo Mapping (PRISM) images from the Advanced Land Observing Satellite (ALOS) acquired in August 2009 and September 2010, and Landsat 8 OLI images acquired in July and August 2014 with open source GIS software QGIS[28]. (5)

Elevation data were interpolated to 1 × 1 m mesh DEMs using the regularized spline with tension method mounted on open source GIS software GRASS GIS[15,29,30]. (6) DEMs were processed to 1 × 1 m mesh grid points and saved as a CSV file. We used MATLAB[31] for procedures (2), (3) and (6). The distance between the reference and rover stations (baseline length) was 3–9004 m for Qaanaaq area and 1–5572 m for Bowdoin Glacier, respectively.

4. Data Records

Surface elevation data are archived at National Institute of Polar Research (for access details, see Data Citation 1). Spatial coverage of the data products is shown for each year in the Qaanaaq (Fig. 3) and Bowdoin Glacier areas (Fig. 4), respectively. Elevation data in Fig. 3 and Fig. 4 are presented for 30-m grid cells by taking a mean of the 1-m resolution GPS data. The processed surface elevation data are stored in a CSV file format. The structure of the data filenames is *place*_*year*_*surface*.csv, where *place* indicates measurement area ("bowdoin" or "qaanaaq"), *year* indicates measured year and *surface* indicates measured surface ("ice" or "land") (Table 1). Data file contains headers in the lines 1–19 as follows; date of data file generation, affiliation, name and contact address of investigators, project name, data file name, data type, statues, observation date, coordinates of GPS reference station (longitude/latitude/elevation), UTM zone, elevation system, delimiter, fields, and units of data. Coordinates in the CSV files are given in longitude (decimal degree), latitude (decimal degree), UTM easting (meter), UTM northing (meter) and elevation (meter) in WGS 84 ellipsoid height.

5. Technical Validation

In this section, we discuss the accuracy of the kinematic GPS measurements. To assess the accuracy of our measurements, two different errors are taken into account: the accuracy of the GPS reference coordinates and the precision of the kinematic measurements. The accuracy of the GPS reference coordinates (σ_{ref}) is given by the standard deviations of the solution computed by the static post-processing. The standard deviations were <0.09 m in the horizontal and <0.14 m in the vertical directions for the reference stations in Qaanaaq Village and Bowdoin Glacier. Uncertainty introduced by re-installation of the GPS antennae (σ_{ref_ant}) was assumed to be <0.01 m in the horizontal and vertical directions. Uncertainty in the vertical position of the rover GPS antenna during the measurements (σ_{rov_ant}) was estimated to be <0.1 m (ref. 13). This uncertainty is due to inclination and vertical movement of the GPS antenna during the survey. The accuracy of GPS rover coordinates (σ_{rov}) is given by the standard deviations of the solution computed by the kinematic post-processing. The standard deviations were <0.09 and <0.18 m in the horizontal and vertical directions, respectively. The total uncertainty in the kinematic GPS measurements were estimated using the law of error propagation:

$$\sigma_{xy} = (\sigma_{ref\_xy}^2 + \sigma_{ref\_ant}^2 + \sigma_{rov\_xy}^2)^{1/2} = 0.13 \text{ m}$$

in the horizontal, and

$$\sigma_z = (\sigma_{ref\_z}^2 + \sigma_{ref\_ant}^2 + \sigma_{rov\_ant}^2 + \sigma_{rov\_z}^2)^{1/2} = 0.25 \text{ m}$$

in the vertical direction. The estimated uncertainties are similar to the values reported for kinematic GPS measurements on glaciers in Svalbard[17], southeastern Himalaya[32,33] and the Southern Patagonia Icefield[34].

6. Usage Notes

This surface elevation product has already been utilized to investigate ice thickness distribution along the flowline of Qaanaaq and Bowdoin Glaciers in combination with ice-radar measurements[23,24]. Based on the thickness data, ice flow and temperature conditions of Qaanaaq Glacier were investigated by applying a thermomechanical-coupled glacier model[23]. Jouvet *et al.*[35] used the data as GCPs for UAV photogrammetry to analyze the flow and calving of Bowdoin Glacier. Tsutaki *et al.*[13] quantified surface elevation changes over Bowdoin Glacier and the adjacent Tugto Glacier. Additionally, our data should help improve understanding of glacier changes in northwestern Greenland when it is combined with remote sending and in-situ observations that may be performed in the future.

7. Competing interests

The authors declare no competing financial interests.

8. Figures

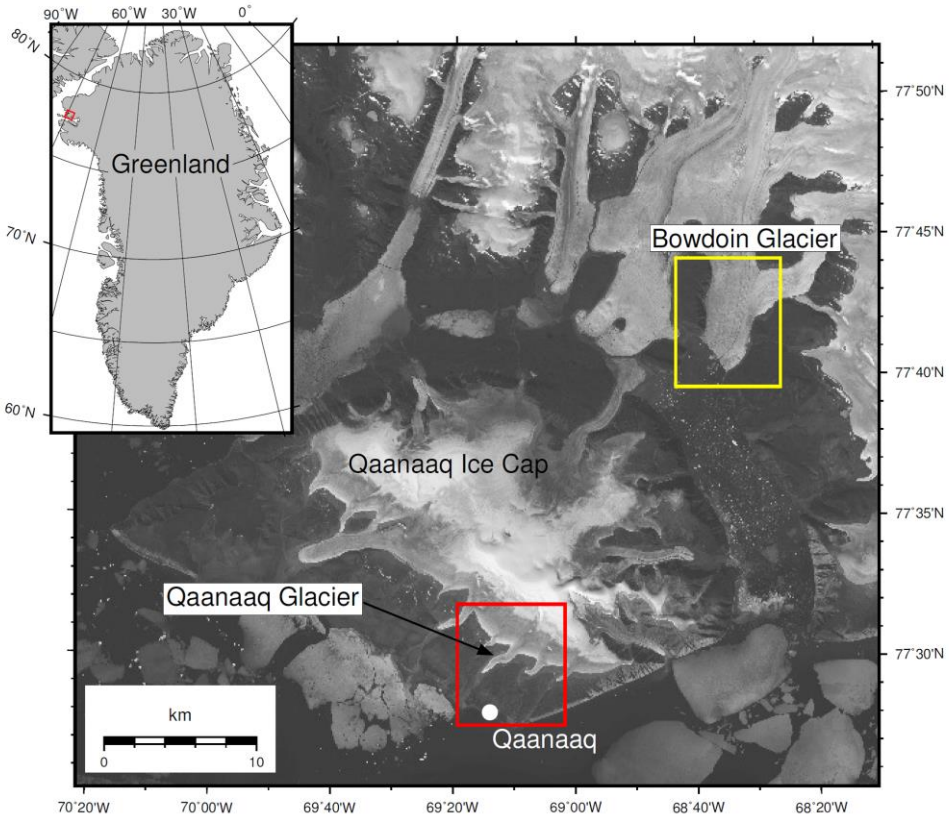

Figure 1. Landsat 8 OLI image (11 July 2015) showing the Qaanaaq region in northwestern Greenland. The red and yellow boxes indicate the areas of study: Qaanaaq and Bowdoin Glaciers. The inset shows the location of the region within Greenland.

Figure 2. GPS reference stations in (a) Qaanaaq Village and (b) Bowdoin Glacier. Kinematic GPS measurements on (c) Qaanaaq Glacier in 2013, and (d) Bowdoin Glacier in 2015.

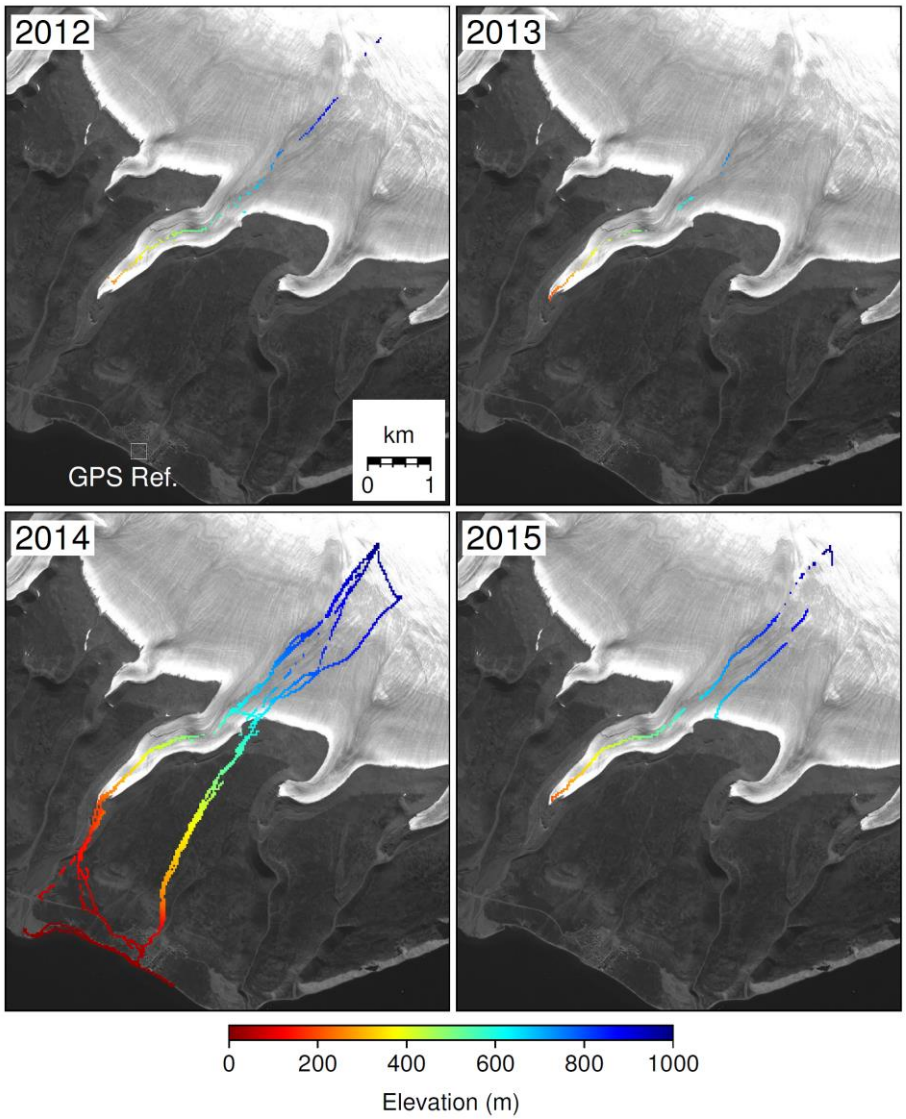

Figure 3. Surface elevation along the survey routes on Qaanaaq Glacier and peripheral ice-free terrain from 2012–2015. Elevation data are averaged every 30 m for the convenience of presentation. The location of the GPS reference station is indicated (square). The background is an ALOS PRISM image taken on 25 August 2009.

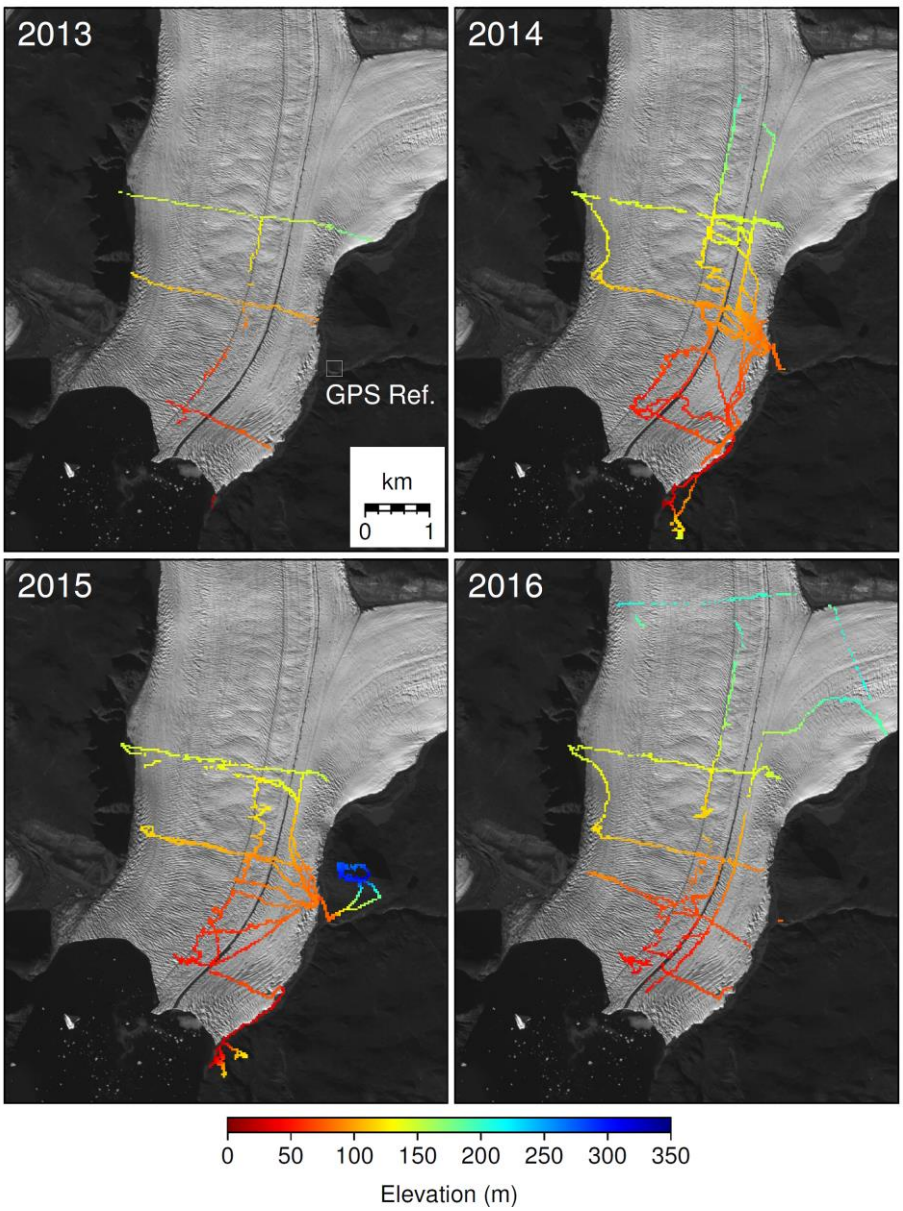

Figure 4. Surface elevation along the survey routes on Bowdoin Glacier and peripheral ice-free terrain from 2013–2016. Elevation data are averaged every 30 m for the convenience of presentation. The location of the GPS reference station is indicated (square). The background is an ALOS PRISM image taken on 4 September 2010.

9. Tables

Table 1. Data files are provided in a CSV file format. The number of data points, GPS survey dates, and survey methods used are indicated.

GPS data filename	Number	Date of GPS survey mm/dd	Methods
bowdoin_2013_ice.csv	654	07/07, 07/09 07/10, 07/11	pole
bowdoin_2013_land.csv	33	07/12	pole
bowdoin_2014_ice.csv	58630	07/12, 07/13, 07/18, 07/19, 07/20, 07/23, 07/24, 07/25	frame pack
bowdoin_2014_land.csv	9189	07/12, 07/13, 07/18, 07/19, 07/20, 07/23, 07/24, 0725	frame pack
bowdoin_2015_ice.csv	30876	07/09, 07/11, 07/13, 07/14, 07/15, 07/16	frame pack
bowdoin_2015_land.csv	10118	07/09, 07/10, 07/11, 07/13, 07/14, 07/15, 07/16	frame pack
bowdoin_2016_ice.csv	19846	07/09, 07/10, 07/11, 07/12, 07/13, 07/15, 07/17, 07/18, 07/19	frame pack
bowdoin_2016_land.csv	4	07/09, 07/14	frame pack
qaanaaq_2012_ice.csv	259	07/26, 07/27, 07/29	pole
qaanaaq_2013_ice.csv	87	07/20, 07/21	pole
qaanaaq_2014_ice.csv	21966	06/17, 06/30, 07/01, 07/07, 08/01, 08/03	frame pack
qaanaaq_2014_land.csv	28203	06/17, 06/30, 07/01, 07/07, 08/01, 08/02, 08/03	frame pack
qaanaaq_2015_ice.csv	6587	07/30	frame pack

Table 2. The coordinates of the GPS reference stations in Qaanaaq Village and Bowdoin Glacier. The horizontal coordinates are described in decimal degree and UTM zone 19X. Elevation is in WGS84 ellipsoid height.

Station name	Longitude	Latitude	UTM Easting	UTM Northing	Elevation
	degree	degree	m	m	m
Qaanaaq	−69.233850646	77.466596715	494334.9748	8598853.9369	27.2951
Bowdoin	−68.507043412	77.684869195	511737.0914	8623250.5517	86.0078

Author contributions

S. Tsutaki and S. Sugiyama designed the study. S. Tsutaki, S. Sugiyama and D. Sakakibara carried out the field measurements. S. Tsutaki and D. Sakakibara performed the post-processing of GPS data. S. Tsutaki performed 1-m mesh grid elevation data generation. All authors contributed in discussion and writing of the manuscript.

Acknowledgements

We thank T. Sawagaki, K. Fujita, S. Matsuno, M. Minowa, M. Maruyama, J. Saito, I. Asaji and the members of the 2012–2016 field campaigns in Qaanaaq for their contributions to the GPS measurements and data processing. Special thanks are due to S. Daorana and T. Ohshima for providing logistical support in Qaanaaq. This research was funded by MEXT (Japanese Ministry of Education, Culture, Sports, Science and Technology) through the Green Network of Excellence (GRENE) Arctic Climate Change Research Project and the Arctic Challenge for Sustainability (ArCS) Project.

References

1. Andersen, M. L. et al. Basin-scale partitioning of Greenland ice sheet mass balance components (2007–2011). Earth Planet. Sci. Lett. 2015, 409, 89–95, https://doi.org/10.1016/j.epsl.2014.10.015.
2. Bolch, T. et al. Mass loss of Greenland's glaciers and ice caps 2003–2008 revealed from ICESat laser altimetry data. Geophys. Res. Lett. 2013, 40(5), 875–881, https://doi.org/10.1002/grl.50270.
3. Sørensen, L. S. et al. Mass balance of the Greenland ice sheet (2003–2008) from ICESat data – the impact of interpolation, sampling and firn density. The Cryosphere. 2011, 5(1), 173–186, https://doi.org/10.5194/tc-5-173-2011.
4. Helm, V., Humbert, A. & Miller, H. Elevation and elevation change of Greenland and Antarctica derived from CryoSat-2. The Cryosphere. 2014, 8(4), 1539–1559, https://doi.org/10.5194/tc-8-1539-2014.
5. Khan, S. A. et al. Sustained mass loss of the northeast Greenland ice sheet triggered by regional warming. Nat. Clim. Chang. 2014, 4(4), 292–299, https://doi.org/10.1038/nclimate2161.
6. Howat, I. M., Joughin, I. & Scambos, T. A. Rapid changes in ice discharge from Greenland outlet glaciers. Science. 2007, 315(5818), 1559–1561, https://doi.org/10.1126/science.1138478.
7. Pritchard, H. D., Arthern, R. J., Vaughan, D. G. & Edwards, L. A. Extensive dynamic thinning on the margins of the Greenland and Antarctic ice sheets. Nature. 2009, 461(7266), 971–975, https://doi.org/10.1038/nature08471.
8. Csatho, B. M. et al. Laser altimetry reveals complex pattern of Greenland Ice Sheet dynamics. Proc. Natl. Acad. Sci. U.S.A. 2014, 111(52), 18478–18483, https://doi.org/10.1073/pnas.1411680112.
9. Simonsen, S. B. & Sørensen, L. S. Implications of changing scattering properties on Greenland ice sheet volume change from Cryosat-2 altimetry. Remote Sens. Environ. 2017, 190, 207–216, https://doi.org/10.1016/j.rse.2016.12.012.
10. Kjær, K. H. et al. Aerial photographs reveal late-20th-century dynamic ice loss in northwestern Greenland. Science. 2012, 337(6094), 569–573, https://doi.org/10.1126/science.1220614.
11. Kjeldsen, K. K. et al. Spatial and temporal distribution of mass loss from the Greenland Ice Sheet since AD 1900. Nature. 2015, 528(7582), 396–400, https://doi.org/10.1038/nature16183.
12. Saito, J., Sugiyama, S., Tsutaki, S. & Sawagaki, T. Surface elevation change on ice caps in the Qaanaaq region, northwestern Greenland. Polar Sci. 2016, 10(3), 239–248, https://doi.org/10.1016/j.polar.2016.05.002.
13. Tsutaki, S., Sugiyama, S., Sakakibara, D. & Sawagaki, T. Surface elevation changes during 2007–13 on Bowdoin and Tugto Glaciers, northwestern Greenland. Journal of Glaciology. 2016, 62(236), 1083–1092, https://doi.org/10.1017/jog.2016.106.
14. Bolch, T., Pieczonka, T. & Benn, D. I. Multi-decadal mass loss of glaciers in the Everest area (Nepal Himalaya) derived from stereo imagery. The Cryosphere. 2011, 5(2), 349–358, https://doi.org/10.5194/tc-5-349-2011.
15. Nuimura, T., Fujita, K., Yamaguchi, S. & Sharma, R. R. Elevation changes of glaciers revealed by multitemporal digital elevation models calibrated by GPS survey in the Khumbu region, Nepal

Himalaya, 1992–2008. Journal of Glaciology. 2012, 58(210), 648–656, https://doi.org/10.3189/2012JoG11J061.

16. Eiken, T., Hagen, J. O. & Melvold, K. Kinematic GPS survey of geometry changes on Svalbard glaciers. Annals of Glaciology. 1997, 24, 157–163, https://doi.org/10.3189/S0260305500012106.
17. Hagen, J. O., Eiken, T., Kohler, J. & Melvold, K. Geometry changes on Svalbard glaciers: mass-balance or dynamic response? Annals of Glaciology. 2005, 42, 255–261, https://doi.org/10.3189/172756405781812763.
18. Whitehead, K., Moorman, B. & Wainstein, P. Measuring daily surface elevation and velocity variations across a polythermal arctic glacier using ground-based photogrammetry. Journal of Glaciology. 2014, 60(224), 1208–1220, https://doi.org/10.3189/2014JoG14J080.
19. Jacobsen, F. M. & Theakstone, W. H. Monitoring glacier changes using a global positioning system in differential mode. Annals of Glaciology. 1997, 24, 314–319, https://doi.org/10.3189/S0260305500012374.
20. James, T. D. et al. Observations of enhanced thinning in the upper reaches of Svalbard glaciers. The Cryosphere. 2012, 6(6), 1369–1381, https://doi.org/10.5194/tc-6-1369-2012.
21. Forsberg, R. et al. Elevation change measurements of the Greenland Ice Sheet. Earth Planets Space. 2000, 52(11), 1049–1053, https://doi.org/10.1186/BF03352329.
22. Matoba, S. et al. Glaciological and meteorological observations at the SIGMA-D site, northwestern Greenland Ice Sheet. Bulletin of Glaciological Research. 2015, 33, 7–14, https://doi.org/10.5331/bgr.33.7.
23. Sugiyama, S. et al. Initial field observations on Qaanaaq ice cap, northwestern Greenland. Annals of Glaciology. 2014, 55(66), 25–33, https://doi.org/10.3189/2014AoG66A102.
24. Sugiyama, S., Sakakibara, D., Tsutaki, S., Maruyama, M. & Sawagaki, T. Glacier dynamics near the calving front of Bowdoin Glacier, northwestern Greenland. Journal of Glaciology. 2015, 61(226), 223–232, https://doi.org/10.3189/2015JoG14J127.
25. Tsutaki, S., Sugiyama, S., Sakakibara, D., Aoki, T. & Niwano, M. Surface mass balance, ice velocity and near-surface ice temperature on Qaanaaq Ice Cap, northwestern Greenland, from 2012 to 2016. Annals of Glaciology. 2017, 1–12, https://doi.org/10.1017/aog.2017.7.
26. JAVAD GNSS Inc. JPS2RIN. 2.0.136. https://javad.com/jgnss/products/software/jps2rin.html, (accessed 2017-09-05).
27. Takasu, T. RTKLIB. 2.4.2. http://www.rtklib.com/, (accessed 2017-09-05).
28. QGIS Development Team. QGIS. 2.18. http://qgis.org/en/site/, (accessed 2017-09-05).
29. GRASS Development Team. GRASS GIS. 7.2.1. https://grass.osgeo.org, (accessed 2017-09-05).
30. Nuimura, T. et al. Temporal changes in elevation of the debris-covered ablation area of Khumbu Glacier in the Nepal Himalaya since 1978. Arct. Antarct. Alp. Res. 2011, 43(2), 246–255.
31. The MathWorks, Inc. MATLAB. R2016b. https://www.mathworks.com/products/matlab.html, (accessed 2017-09-05).

32. Fujita, K., Suzuki, R., Nuimura, T. & Sakai, A. Performance of ASTER and SRTM DEMs, and their potential for assessing glacial lakes in the Lunana region, Bhutan Himalaya. Journal of Glaciology. 2008, 54(185), 220–228, https://doi.org/10.3189/002214308784886162.
33. Wagnon, P. et al. Seasonal and annual mass balances of Mera and Pokalde glaciers (Nepal Himalaya) since 2007. The Cryosphere. 2013, 7(6), 1769–1786, https://doi.org/10.5194/tc-7-1769-2013.
34. Raymond, C. et al. Retreat of Glaciar Tyndall, Patagonia, over the last half-century. Journal of Glaciology. 2005, 51(173), 239–247, https://doi.org/10.3189/172756505781829476.
35. Jouvet, G. et al. Initiation of a major calving event on the Bowdoin Glacier captured by UAV photogrammetry. The Cryosphere. 2017, 11(2), 911–921, https://doi.org/10.5194/tc-11-911-2017.

Data Citations

1. Tsutaki, S., Sugiyama, S. & Sakakibara, D. Surface elevations on Qaanaaq and Bowdoin Glaciers in northwestern Greenland as measured by a kinematic GPS survey from 2012-2016. 1.00, Japan, Arctic Data archive System (ADS), 2017. https://doi.org/10.17592/001.2017060801.